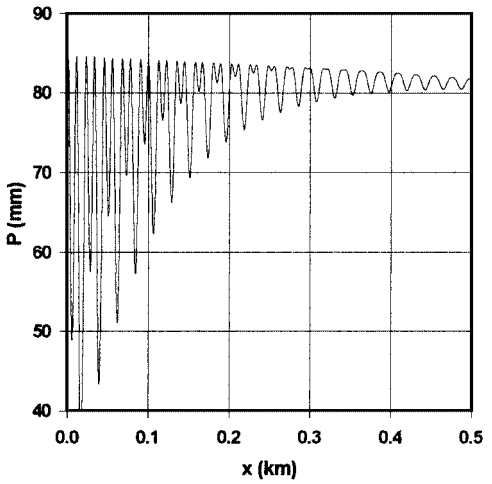

Fig. 2 Perforation into oblique plate.

Oblique Target

In actual usage, normal incidence targets are rarely encountered. Tank frontal armors are highly sloped, and engagements occur at arbitrary angles between combatants. Roecker and Grabarek[7] present data for penetration of yawed tungsten alloy rods into semi-infinite RHA targets at obliquities of 60, 65, and 70 deg. Data are given only in the pitch plane, i.e., the plane containing the surface normal of the plate and the velocity vector of the rod. Examination shows that it is difficult to ascertain a meaningful difference between the data at various obliquities. For this reason, the data are grouped into a single set and fit to the relation

$$P/P_0 = \cos(12.59\alpha - 7.81) \tag{5}$$

To treat combined pitch and yaw, it is necessary to make some assumptions that are not supported by the available data set. It will be assumed that the degradation of perforation due to yaw alone into the oblique plate can be represented by Eq. (3), with P_0 given by Eq. (1). It will further be assumed that the pitch and yaw effects can be separated using the following relation:

$$\frac{P}{P_0} = \cos(12.59\alpha - 7.81)\cos\left(\frac{11.46\beta}{\beta_{\text{crit}}}\right) \tag{6}$$

Whereas this expression cannot be proven to be valid for the oblique plate, this type of separation can be shown to be a reasonable approximation in the case of normal incidence impact if the total yaw is less than 5 deg. Equations (1), (2), and (4–6) permit the calculation of perforation vs range for combined pitching and yawing motion. With the plane of angular motion oriented 45 deg (equal pitch and yaw) from the vertical, the thickness of $\theta = 65$ deg oblique RHA perforated is plotted in Fig. 2. The plot clearly shows the influence of the pitch plane perforation asymmetry, Eq. (5). As the round moves downrange, the perforation is more severely degraded by the adverse pitch states. The reason that the values of P are so much lower in this case is that Eq. (1) gives the thickness of plate perforated, not the line-of-sight perforation.

Conclusions

A method to estimate the effects of free-flight drag and angular motion on perforation is presented. Both normal and oblique impacts are treated. Predictions show that, at discrete ranges, penetrator performance is significantly degraded by angular motion. As range increases, yaw damps, and deceleration due to aerodynamic drag dominates.

References

[1]Hohler, V., and Stilp, A. J., "Penetration of Steel and High Density Rods into Semi-Infinite Steel Targets," *Proceedings of the 3rd International Symposium on Ballistics*, National Defense Industrial Association, Paper H3, Arlington, VA, 1977.

[2]Lanz, W., and Odermatt, W., "Penetration Limits of Conventional Large Caliber Anti Tank Guns/Kinetic Energy Projectiles," *Proceedings of the 13th International Symposium on Ballistics*, Vol. 3, National Defense Industrial Association, Arlington, VA, 1992, pp. 227–236.

[3]Bjerke, T., Silsby, G., Scheffler, D., and Mudd, R., "High Yaw Penetration Performance of Long Rod Penetrators," *Proceedings of the 13th International Symposium on Ballistics*, Vol. 3, National Defense Industrial Association, Arlington, VA, 1992, pp. 201–208.

[4]Reinecke, W., "Novel Kinetic Energy Projectiles for Hypervelocity Anti-Armor Applications," AIAA Paper 97-0483, Jan. 1997.

[5]Mikhail, A., "In-Flight Flexure and Spin Lock-In for Kinetic Energy Projectiles," AIAA Paper 95-3429, Aug. 1995.

[6]Murphy, C. H., "Free Flight Motion of Symmetric Missiles," U.S. Army Ballistic Research Lab., BRL Rept. 1216, Aberdeen Proving Ground, MD, July 1963.

[7]Roecker, E., and Grabarek, C., "The Effect of Yaw and Pitch on Long Rod Penetration into Rolled Homogeneous Armor at Various Obliquities," *Proceedings of the 9th International Symposium on Ballistics*, Vol. 2, National Defense Industrial Association, Arlington, VA, 1986, pp. 467–473.

R. M. Cummings
Associate Editor

Numerical Study of Hypersonic Rarefied-Gas Flows About a Torus

Vladimir V. Riabov*
University of New Hampshire, Manchester, New Hampshire 03101

Nomenclature

A	= torus base area, $4\pi RH$, m^2
C_f	= local skin-friction coefficient, $\tau_w/q_\infty A$
C_p	= local pressure coefficient, $(p_w - p_\infty)/q_\infty A$
C_x	= drag coefficient
H	= distance between the axis of symmetry and the torus disk center, m
$Kn_{\infty,R}$	= Knudsen number
M	= Mach number
p	= pressure, N/m^2
q_∞	= dynamic pressure, $0.5\rho_\infty u_\infty^2$, N/m^2
R	= radius of a torus disk, 0.1 m
τ_w	= viscous stress at the torus surface, N/m^2

Subscripts

R	= torus disk radius as a length-scale parameter
w	= wall condition
∞	= freestream parameter

Introduction

NUMERICAL and experimental studies of the aerothermodynamics of simple-shape bodies have provided valuable information related to physics of hypersonic flows about spacecraft elements and testing devices.[1–5] Numerous results had been found in the cases of plates, wedges, cones, disks, spheres, and cylinders.[1–7]

In the present study, the hypersonic rarefied-gas flow about a torus has been studied. The flow pattern has not been yet discussed in the research literature. Several features of the flow are unique.

Presented as Paper 98-0778 at the AIAA 36th Aerospace Sciences Meeting, Reno, NV, Jan. 12–15, 1998; received April 8, 1998; revision received Sept. 28, 1998; accepted for publication Sept. 29, 1998.

*Lecturer, College of Engineering and Physical Sciences, 400 Commercial Street. Member AIAA.

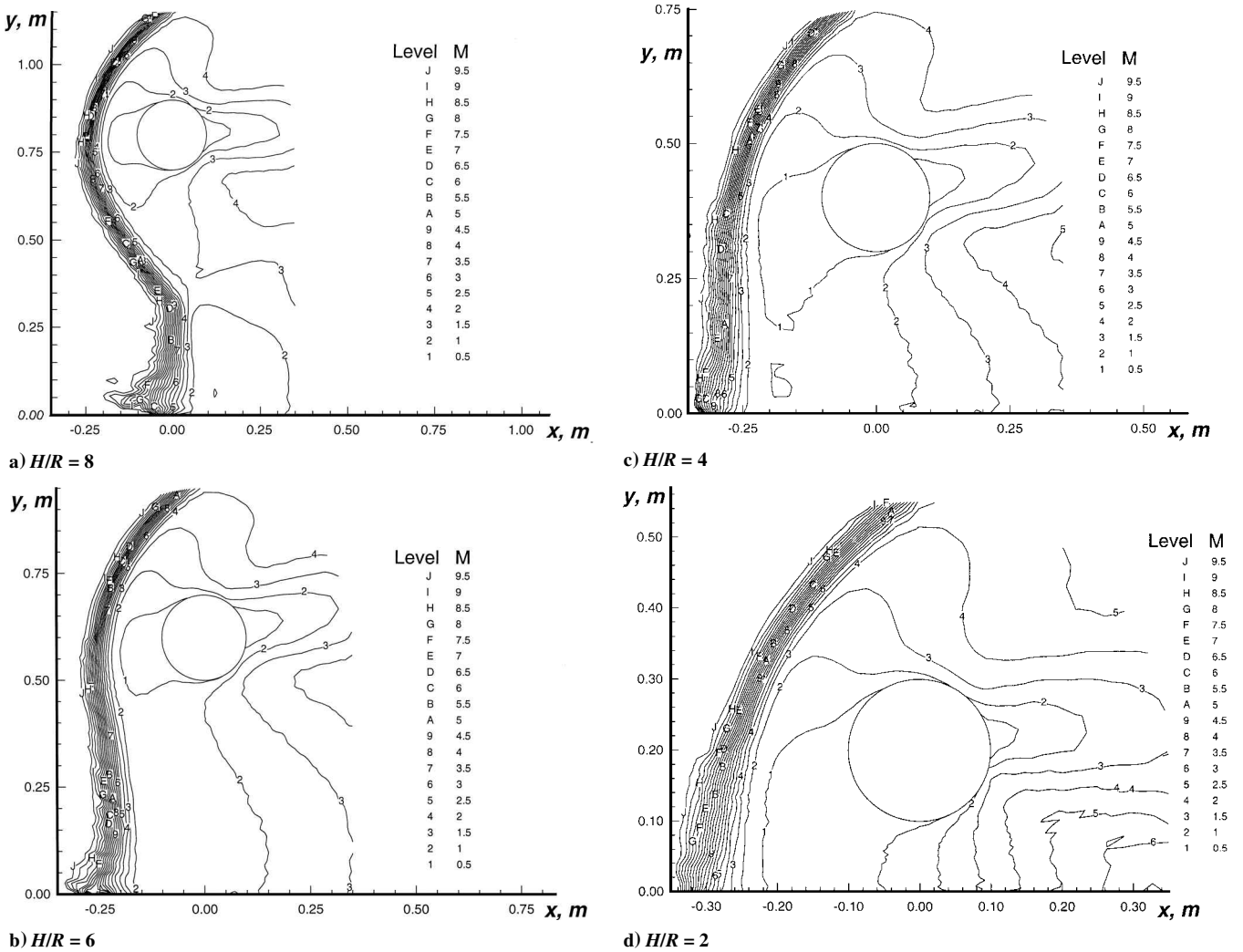

Fig. 1 Mach number contours in argon flow about a torus at $Kn_{\infty,R} = 0.1$ and $M_\infty = 10$.

For example, if the distance between the axis of symmetry and the torus disk center H is significantly larger the torus radius R, then the flow can be approximated by a stream between two side-by-side cylinders.[8] At $H = R$, the rarefied gas flow has some features of a stream near a bluff disk. In the first case, two conical shock waves would focus and interact in the vicinity of the symmetry axis generating the normal shock wave and the conical reflected waves. The stagnation points would be near the front points of the torus disks. In the second case, the front shock wave would be normal, and the location of stagnation points would be difficult to predict. At $H > R$, the flow pattern and shock-wave shapes are very complex. As a result, simple approximation techniques would not be applied in torus aerothermodynamics.

Flow about a torus and its aerodynamic characteristics have been studied under the conditions of a hypersonic rarefied-gas stream at $8R \geq H \geq 2R$ and Knudsen number $Kn_{\infty,R}$ from 0.0167 to 1. The numerical results have been obtained using the direct simulation Monte Carlo (DSMC) technique.[3] The computer code was developed by Bird.[9]

DSMC Method

The DSMC method[3] is used as a numerical simulation technique for low-density hypersonic gas flows. An axisymmetrical DSMC code[9] is used. Molecular collisions in argon are modeled using the variable hard sphere molecular model.[3] The gas–surface interactions are assumed to be fully diffusive with full moment and energy accommodation. The code validation was tested by the author[5] in comparing numerical results with experimental data[4,5] related to the simple-shape bodies.

In calculations at $H/R = 8$, the total number of cells near a torus (a half-space of the unit segment) is 3000 in three zones, the molecules are distributed nonevenly,[2] and a total number of 27,200 molecules corresponds to an average of 9 molecules per cell. Following the recommendations of Refs. 2, 3, and 9, acceptable results are obtained for an average of at least 10 molecules per cell in the most critical region of the flow. The error was pronounced when this number fell below five, i.e., flow near the symmetry axis (Figs. 1a and 1b). In all cases the usual criterion[2] for the time step Δt_m has been realized: $2 \times 10^{-7} \leq \Delta t_m \leq 1 \times 10^{-6}$ s. Under these conditions, aerodynamic coefficients and gasdynamic parameters have become insensitive to the time step.

The location of the external boundary with the upstream flow conditions varies from $2.5R$ to $3.5R$. Calculations were carried out on a personal computer. The computing time of each variant was estimated to be approximately 10–60 h.

Results

Influence of the Geometrical Factor H/R

The flow pattern over a torus is significantly sensitive to the major geometrical similarity parameter H/R. The influence of this parameter on the flow structure has been studied for hypersonic flow of argon at $M_\infty = 10$ and $Kn_{\infty,R} = 0.1$. It is assumed that the wall temperature is equal to the stagnation temperature.

The local Mach number contours are shown in Fig. 1 for four cases of the geometrical factor ($H/R = 8, 6, 4$, and 2). At $H/R = 8$, a conical shock wave can be observed near the torus. The interference of the shock waves takes the form of the normal shock wave (the Mach disk) in the vicinity of the symmetry axis. At the intersection of the

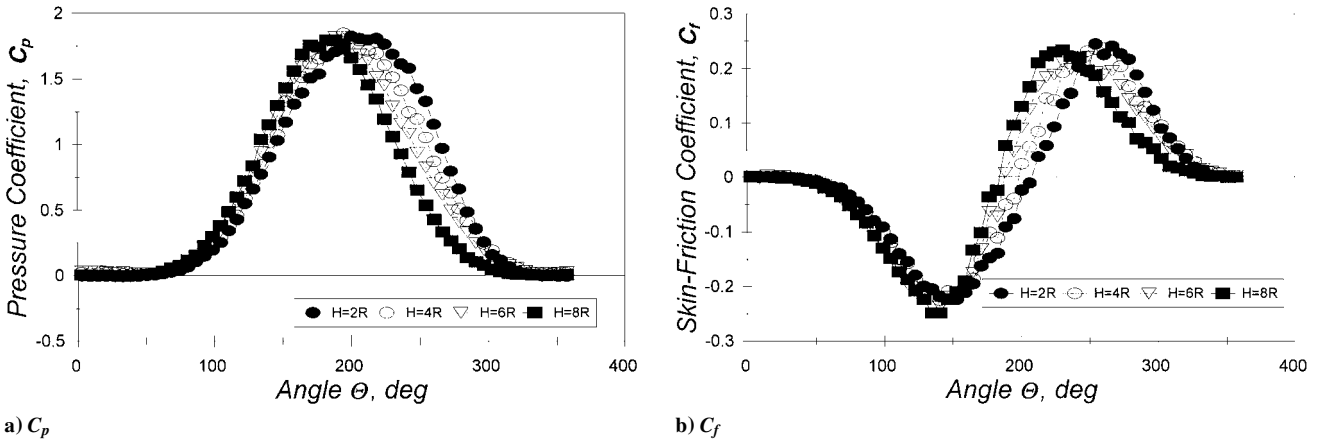

a) C_p b) C_f

Fig. 2 Pressure and skin-friction coefficients along the torus surface at $Kn_{\infty,R} = 0.1$ and $M_\infty = 10$.

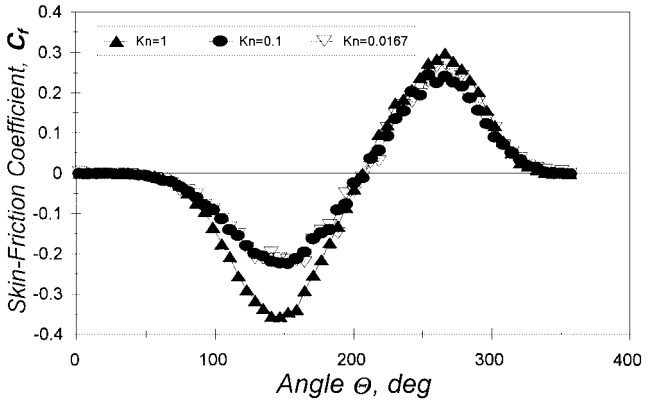

Fig. 3 Skin-friction coefficient C_f along the torus surface at $H/R = 2$ and $M_\infty = 10$.

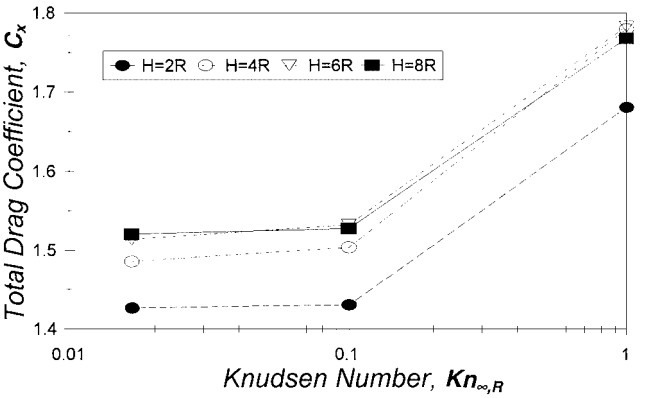

Fig. 4 Total drag coefficient of the torus vs Knudsen number $Kn_{\infty,R}$ at $M_\infty = 10$.

conical and normal shock waves, a new type of conical reflection wave has been found. This internal reflection wave is observed in density, temperature, and velocity contour diagrams.[10] The boundaries of a local subsonic zone are restricted by supersonic conical flow behind the conical shock waves and the reflected waves.

The shock-wave shape and the scale of the subsonic zone behind the shock wave are very sensitive to the geometrical parameter H/R (Fig. 1). At $H/R \leq 4$, the shape of a front shock wave becomes normal, and the subsonic area is restricted by the location of the shock wave and the torus throat (Figs. 1c and 1d). This effect plays a fundamental role in the redistribution of pressure and skin friction along the torus surface [Figs. 2a and 2b, correspondingly; the angle θ changes from the torus rear point ($\theta = 0$ deg) in the counterclockwise direction].

The dynamics of the subsonic zone is a major factor of relocation of the stagnation-point ring in the front area of the torus. The location of the stagnation point is moving from the front area to the torus throat after reducing the outer torus radius. The identical effect can be observed in calculations of pressure and skin-friction coefficients (Fig. 2).

Influence of the Knudsen Number $Kn_{\infty,R}$

The rarefaction factor, which can be characterized by the Knudsen number $Kn_{\infty,R}$, plays an important role in the flow structure[3,5–7] as well as in aerodynamics.[1,4,5] The flowfield about a torus has been calculated for the hypersonic flow of argon at $M_\infty = 10$ and Knudsen numbers $Kn_{\infty,R} = 0.0167$, 0.1, and 1.

Under continuum flow conditions ($Kn_{\infty,R} = 0.0167$), the flow structure has the same features as were discussed earlier. In the transitional flow regime, at $Kn_{\infty,R} = 1$, the flow pattern is different.[10] The reflection waves have different shapes because of the rarefaction effects in the conic and normal shock waves. At a small outer torus radius, $H/R = 2$, the skin-friction coefficient distribution along the torus surface becomes sensitive to the rarefaction parameter $Kn_{\infty,R}$ (Fig. 3). The locations of the front stagnation points are not changed at different Knudsen numbers.

The calculating results of the total drag coefficient are shown in Fig. 4. At any outer–inner radii ratio, the drag coefficient increases with increasing Knudsen number. The geometrical factor becomes insignificant on the drag at $H/R \geq 6$ under continuum flow regime conditions and at $H/R \geq 4$ in the free-molecule flow regime.

Conclusion

The hypersonic rarefied-gas flow about a torus has been studied by the DSMC technique. The flow pattern and shock-wave shapes are significantly different for small and large inner-outer radii ratios. At a value of the geometrical ratio parameter H/R of 8, the conical shock waves interact in the vicinity of the symmetry axis, creating the normal shock wave (the Mach disk). The reflected conical wave has a different pattern of the interaction with the supersonic flow behind a torus in continuum and rarefied-gas flow regimes.

At the small-ratio parameters, the front shock-wave shape becomes normal, and the front stagnation points relocate from the torus front zone toward the throat area. This phenomenon affects the drag, pressure, and skin-friction distributions along the torus.

Acknowledgments

The author would like to express gratitude to G. A. Bird for the opportunity of using the DS2G computer program and to J. N. Moss for valuable discussions of the technique and results.

References

[1] Koppenwallner, G., and Legge, H., "Drag of Bodies in Rarefied Hypersonic Flow," *Thermophysical Aspects of Re-Entry Flows*, edited by C. D. Scott and J. N. Moss, Vol. 103, Progress in Astronautics and Aeronautics, AIAA, Washington, DC, 1994, pp. 44–59.

[2]Bird, G. A., "Rarefied Hypersonic Flow Past a Slender Sharp Cone," *Proceedings of the 13th International Symposium on Rarefied Gas Dynamics*, Vol. 1, Plenum, New York, 1985, pp. 349–356.

[3]Bird, G. A., *Molecular Gas Dynamics and the Direct Simulation of Gas Flows*, 1st ed., Oxford Univ. Press, Oxford, England, UK, 1994, pp. 340–377.

[4]Gusev, V. N., Erofeev, A. I., Klimova, T. V., Perepukhov, V. A., Riabov, V. V., and Tolstykh, A. I., "Theoretical and Experimental Investigations of Flow over Simple Shape Bodies by a Hypersonic Stream of Rarefied Gas," *Trudy TsAGI*, No. 1855, 1977, pp. 3–43 (in Russian).

[5]Riabov, V. V., "Comparative Similarity Analysis of Hypersonic Rarefied Gas Flows Near Simple-Shape Bodies," *Journal of Spacecraft and Rockets*, Vol. 35, No. 4, 1998, pp. 424–433.

[6]Gorelov, S. L., and Erofeev, A. I., "Qualitative Features of a Rarefied Gas Flow About Simple Shape Bodies," *Proceedings of the 13th International Symposium on Rarefied Gas Dynamics*, Vol. 1, Plenum, New York, 1985, pp. 515–521.

[7]Lengrand, J. C., Allège, J., Chpoun, A., and Raffin, M., "Rarefied Hypersonic Flow over a Sharp Flat Plate: Numerical and Experimental Results," *Rarefied Gas Dynamics: Space Science and Engineering*, edited by B. D. Shizdal and D. P. Weaver, Vol. 160, Progress in Astronautics and Aeronautics, AIAA, Washington, DC, 1994, pp. 276–284.

[8]Blevins, R. D., *Applied Fluid Dynamics Handbook*, Krieger, Malabar, FL, 1992, pp. 318–333.

[9]Bird, G. A., "The DS2G Program User's Guide, Version 1.0," G. A. B. Consulting Pty, Killara, NSW, Australia, 1995, pp. 1–50.

[10]Riabov, V. V., "Numerical Study of Hypersonic Rarefied-Gas Flow About a Torus," AIAA Paper 98-0778, Jan. 1998.

I. D. Boyd
Associate Editor

Errata

Influence of X-Ray Solar Flare Radiation on Degradation of Teflon® in Space

Andrei Milintchouk, Marc Van Eesbeek, François Levadou, and Tim Harper
European Space Agency, 2200 AG Noordwijk, The Netherlands
[J. Spacecraft, 34(4), pp. 542–548 (1997)]

BECAUSE of an editing error, incorrect units were given for the estimate of energy deposited by solar flares in a 20-μm-thick FEP film on LDEF. At the top of the second column on page 547, the dosage should read 10^5–10^6 rad, not 10^5–10^6 Gy. AIAA regrets the error.